Low-resistance ohmic contacts to *p*-type GaN achieved by the oxidation of Ni/Au films

Jin-Kuo Ho,[a] Charng-Shyang Jong, Chien C. Chiu, Chao-Nien Huang, and Kwang-Kuo Shih
Opto-Electronics and Systems Laboratories, Industrial Technology Research Institute, Hsinchu, Taiwan 310, Republic of China

Li-Chien Chen, Fu-Rong Chen, and Ji-Jung Kai
Department of Engineering and System Science, National Tsing Hua University, Hsinchu, Taiwan 300, Republic of China

(Received 15 March 1999; accepted for publication 7 July 1999)

A contact has been developed to achieve a low specific contact resistance to *p*-type GaN. The contact consisted of a bi-layer Ni/Au film deposited on *p*-type GaN followed by heat treatment in air to transform the metallic Ni into NiO along with an amorphous Ni–Ga–O phase and large Au grains. A specific contact resistance as low as $4.0\times10^{-6}\ \Omega\ \mathrm{cm}^2$ was obtained at 500 °C. This low value was obtained by the optimization of Ni/Au film thickness and heat treatment temperatures. Below about 400 °C, Ni was not completely oxidized. On the other hand, at temperatures higher than about 600 °C, the specific contact resistance increased because the NiO detached from *p*-GaN and the amount of amorphous Ni–Ga–O phase formed was more than that of the sample annealed at 500 °C. The mechanism of obtaining low-resistance ohmic contacts for the oxidized Ni/Au films was explained with a model using energy band diagrams of the Au/*p*-NiO/*p*-GaN structure. © *1999 American Institute of Physics.* [S0021-8979(99)00820-8]

I. INTRODUCTION

Group III nitride semiconductors have attracted great attention in recent years owing to the successful commercialization of light emitting diodes from ultraviolet to visible range[1–5] and the development of laser diodes with a lifetime longer than 10 000 h.[6] Meanwhile, various kinds of devices based on these materials have also been developed, including ultraviolet photoconductive[7,8] and ultraviolet photovoltaic detectors,[9] heterojunction phototransistors,[10] metal-semiconductor field effect transistors,[11] heterostructure field effect transistors,[12] modulation doped field effect transistors,[13] and heterojunction bipolar transistors.[14] Low-resistance ohmic contact to GaN is essential to the performance of these devices.

Previous studies have demonstrated ohmic contact to *n*-GaN with specific contact resistance (ρ_c) as low as 10^{-6}–$10^{-8}\ \Omega\ \mathrm{cm}^2$ by using Ti/Al/Ni/Au[15] or Ti/Al/Pt/Au[16] contacts with proper surface pretreatment of GaN. Currently, Ti/Al based metallization schemes are widely used for *n*-GaN contacts. The formation of the reaction products such as Al–Ti intermetallics,[17,18] TiN[18,19] and AlN[19,20] was proposed to explain the mechanism of obtaining low ρ_c. However, low-resistance ohmic contact to *p*-GaN so far has had little success with reported ρ_c values greater than $10^{-4}\ \Omega\ \mathrm{cm}^2$. These higher values are inappropriate for high performance devices having small contact areas.

The difficulties in achieving low-resistance ohmic contacts to *p*-GaN are due to the fact that the carrier concentration of *p*-GaN cannot be increased to a degenerate level during epitaxial growth, and a practical metal with a higher work function than that of *p*-GaN is not available. Mg is typically used as a *p*-type dopant with an activation energy of about 170 meV,[21,22] which is very low compared to other acceptors. However, this activation energy is still too high, implying that only about 1% of Mg dopants ionize at room temperature when the doped Mg concentration is $10^{20}\ \mathrm{cm}^{-3}$. Meanwhile, the formation of Mg–H complexes further reduces the carrier concentration. Therefore, the carrier concentration of the *p*-GaN layer is limited to a value less than mid $10^{18}\ \mathrm{cm}^{-3}$.[1,23] Diffusion[24,25] and ion implantion[26–29] were studied to increase the carrier concentration, but did not reveal any significant improvement. Metals with a high work function were chosen to obtain low-resistance ohmic contacts, e.g., Au,[30,31] Ni,[30,32] Pd,[33] Pt,[30,34] Ni/Au,[34–39] Pt/Au,[34,38] Cr/Au,[37] Pd/Au,[37,38,40] Pd/Pt/Au,[34] Ni/Cr/Au,[35] Ni/Pt/Au,[41,42] and Pt/Ni/Au.[42,43] The semiconductor's surface condition prior to metal deposition also influenced the contact. A very thin layer of native oxide could severely degrade it. Conversely, the reduction of surface contamination also reduced ρ_c.[36,40] Unfortunately, the lowest reported value of ρ_c with proper surface pretreatment of *p*-GaN was only $4\times10^{-4}\ \Omega\ \mathrm{cm}^2$. Since using a metal with a high work function cannot obtain an ohmic contact of the required quality, the concept of solid phase reaction proposed by Sands, Marshall, and Wang[44] was employed. This approach incorporated *p*-type dopants into the semiconductor superficial layer to produce a low-resistance contact. Mg and Zn were categorized to shallow *p*-type doping elements, hence, these dopants were added into the contact metal. Although metallization schemes including Au/Mg/Au,[31] Ni/Mg/Ni/Si,[45] Ni/Au–Zn,[46,47] and Cr/Au–Zn,[47] were investigated, no evi-

[a]Electronic mail: jinkuo@itri.org.tw

 © 1999 American Institute of Physics

Downloaded 08 Apr 2004 to 128.200.94.51. Redistribution subject to AIP license or copyright, see http://jap.aip.org/jap/copyright.jsp

dent progress was made in decreasing ρ_c with ρ_c limited to $10^{-3}\ \Omega\,\mathrm{cm}^2$ range. Recently, Suzuki *et al.*[48] proposed that metals having strong binding energies with hydrogen atoms can make low-resistance ohmic contacts to p-GaN because the metals can attract the hydrogen atoms from p-GaN at high temperatures to increase the hole concentration of p-GaN. The use of Ta/Ti as the metal contact obtained a ρ_c as low as $3\times10^{-5}\ \Omega\,\mathrm{cm}^2$. Unfortunately, this contact is unstable in air.

Another approach to achieving low-resistance ohmic contact is through semiconductor band gap engineering. Small band gap semiconductors can promote thermionic emission of carriers. Thus thin, heavily doped cap layers of small band gap semiconductors have been applied to various devices to obtain low contact resistance InN, having a lower band gap than GaN and AlN, should produce a lower contact resistance when a layer of InN or InGaN is built on GaN. Although the *n*-type InGaN/GaN epitaxial structure supports this notion,[49] no actual reports on p-GaN have yet been carried out. Another possibility for making low-resistance contacts by band gap engineering is to construct a superlattice structure that combines a top layer with the well material. Tests with n-GaN using an InN/GaN strained superlattice and an InN cap layer have verified that this approach works.[50] However, its effectiveness given p-GaN has not been tested.

Recently, Ho *et al.*[51] reported a method to obtain an ohmic contact to p-GaN with ρ_c lower than $1.0\times10^{-4}\ \Omega\,\mathrm{cm}^2$. Ni/Au metal films were deposited on p-GaN and then heat treated in an oxidizing ambient at temperatures between 400 and 500 °C. Ni transformed to NiO, while Au remained in the metallic state. That investigation conjectured that the creation of low-resistance ohmic contact is attributed to the formation of *p*-type NiO. Cross-sectional transmission electron microscope analysis revealed that the as-deposited Au film converted into discontinuous islands connected with p-GaN.[52] Besides crystalline NiO, an amorphous Ni–Ga–O phase was also present at the interface between the contact and p-GaN. These results suggest that the crystalline NiO and/or amorphous Ni–Ga–O phase may play a significant role in lowering ohmic contact resistance to p-GaN. NiO, which is a *p*-type semiconductor, may serve as a medium between p-GaN and metal in forming ohmic contacts. In this investigation, we achieve ρ_c with a value as low as $4\times10^{-6}\ \Omega\,\mathrm{cm}^2$ by adjusting the Ni/Au thickness. In order to understand the mechanism for obtaining low contact resistance to p-GaN, a model based on energy band diagram is also proposed to explain the results which will be discussed below.

II. EXPERIMENTAL PROCEDURES

The GaN samples used in this study were grown by a low pressure metalorganic chemical vapor deposition method on (0001) sapphire substrates. The substrates were cleaned with organic solvents before loading into the chemical vapor deposition system. A thin GaN nucleation layer was initially grown on sapphire at low temperatures, followed by a 2-μm-thick undoped GaN and 2-μm-thick Mg doped GaN at about 1000 °C. During GaN growth, trimethylgallium, ammonia, and bis-cyclopentadienyl magnesium were used as Ga, N, and Mg sources, respectively. The carrier gas was H_2. The undoped GaN was inherent *n*-type with carrier concentration of $1\times10^{17}\ \mathrm{cm}^{-3}$, and the hole concentration of the Mg doped p-GaN was $2\times10^{17}\ \mathrm{cm}^{-3}$ after heat treating in a nitrogen atmosphere. The average surface roughness measured with a stylus surface profilemeter was below 10 nm. The GaN epilayers measured had about 200 arcsec of full width at half maximum of (0002) diffraction in the rocking curve x-ray diffraction (XRD) analysis.

The specific contact resistance was characterized by current–voltage ($I-V$) measurements based on the circular transmission line model (CTLM).[53,54] For the CTLM measurement, the total resistance, R_t, between two contacts separated by a circular gap is given by Eq. (1)

$$R_t=\frac{R_{\mathrm{sh}}}{2\pi}\times\left[\ln\left(\frac{R}{r}\right)+L_t\left(\frac{1}{R}+\frac{1}{r}\right)\right], \tag{1}$$

where R_{sh} denotes the sheet resistance of p-GaN, R and r represent the radius of the outer and inner circular contact, respectively, and L_t is the transfer length. The total resistance was measured for various spacings and plotted as function of $\ln(R/r)$. The least squares curve fitting method was used to obtain a straight line plot of R_t vs $\ln(R/r)$ data. The slope leads to R_{sh}, and the intercept at $\ln(R/r)=0$ is $R_{\mathrm{sh}}\cdot L_t/r\pi$, giving L_t. Thus, the specific contact resistance, ρ_c, can be obtained by Eq. (2)

$$L_t=\sqrt{\frac{\rho_c}{R_{\mathrm{sh}}}}. \tag{2}$$

The CTLM pattern was designed with a constant inner radius $r=150\ \mu$m and spacings of 14, 17, 20, 26, 32, 40, 50, and 70 μm. The CTLM pattern was transferred to metal films by the conventional thin film deposition and photolithographic lift-off processes. Prior to metal deposition the samples were etched with $HCl{:}H_2O=1{:}1$ for 1 min to remove native oxides. The Ni and Au films were deposited consecutively using an electron beam evaporation system with a base pressure lower than 3×10^{-6} Torr. The metallized samples were heat treated in a hot wall furnace with a flow of air or oxygen for 10 min. The phase formation during heat treatment was analyzed by conducting XRD. Microstructure and crystal structure were analyzed in detail with a high resolution field emission gun transmission electron microscope (TEM). The tripod polishing method was used to prepare cross-sectional TEM samples. Finally, the TEM samples were mounted on Cu grids and then ion milled.

III. RESULTS

$I-V$ measurements on CTLM patterned samples revealed that all the $I-V$ curves of as-deposited Ni/Au contacts to p-GaN exhibited nonlinear characteristics, indicating a Schottky-type barrier between contact and p-GaN. The rectified behavior did not change by using postdeposition heat treatment in nitrogen or forming gas. However, the $I-V$ curves became linear indicating the formation of an ohmic interface after heat treating in air or pure oxygen ambient in

Downloaded 08 Apr 2004 to 128.200.94.51. Redistribution subject to AIP license or copyright, see http://jap.aip.org/jap/copyright.jsp

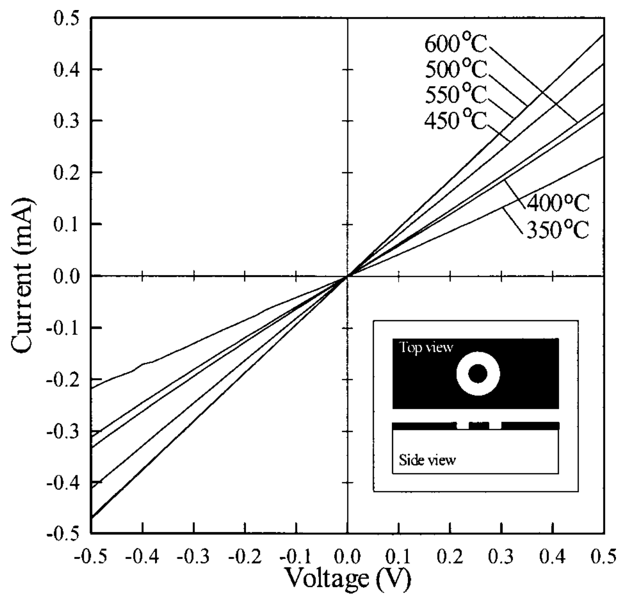

FIG. 1. CTLM $I-V$ measurement of Ni (5 nm)/Au (5 nm) contacts to p-GaN heat treated at 500 °C for 10 min in air. The spacing is 14 μm. The inset at lower right indicates the pattern of CTLM measurement.

the temperature range of about 300–600 °C. Figure 1 displays the results of $I-V$ measurement for the samples with Ni (5 nm)/Au (5 nm) contacts heat treated in air. There were no obvious differences in R_t for the samples heat treated at the same temperatures in either an air or oxygen atmosphere. To determine ρ_c, data on R_t obtained from Fig. 1 were plotted as a linear function of ln(R/r) in Fig. 2. The slopes produced closely resembled each other. The difference in the R_{sh} values obtained from CTLM measurements and those

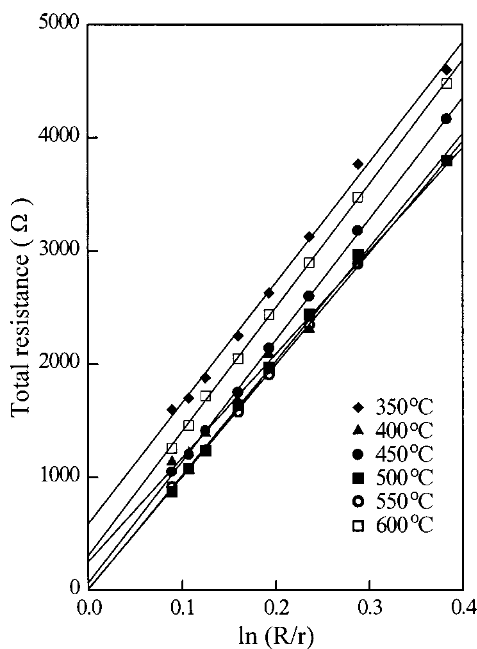

FIG. 2. The dependence of R_t on ln(R/r) for the oxidized Ni (5 nm)/Au (5 nm) contacts to p-GaN.

from Hall measurements was less than 8.7%. Hence, we believe that ρ_c obtained from our CTLM analysis appears to be reliable.

The $I-V$ curves of the samples heat treated in air at temperatures below approximately 350 °C showed a nonlinear behavior which was similar to those heat treated in nitrogen. In addition, the ρ_c of many samples could not be obtained because R_t did not exhibit a linear function with respect to ln(R/r). This phenomenon could result from incomplete and/or inhomogeneous oxidation of Ni. Certainly, XRD analysis indicated that large amounts of Ni still existed in the contact layers. Under such condition, ρ_c was determined to be in the range of $10^{-1}-10^{-2}\ \Omega\ \mathrm{cm}^2$ when R_t was defined at 0.5 V forward bias that current flows into the center circular contacts.

Figure 3 displays the variation of ρ_c as a function of heat treatment temperature in air for Ni/Au contacts with various combinations of Ni/Au thickness. This figure does not contain those contacts with asymmetric $I-V$ curves. The slopes of the curves reveal that ρ_c heavily depended on both heat treatment temperature and Ni/Au film thickness. In general, ρ_c initially decreased with increasing heat treatment temperature, and subsequently increased. A minimum $\rho_c = 4 \times 10^{-6}\ \Omega\ \mathrm{cm}^2$ was obtained for the Ni (5 nm)/Au (5 nm) contact heat treated at 500 °C. Another contact Ni (20 nm)/Au (20 nm), also heat treated at 500 °C, also exhibited low $\rho_c = 8 \times 10^{-6}\ \Omega\ \mathrm{cm}^2$, as shown in Fig. 3(b). Apparently, low-resistance ohmic contact could be achieved when the Ni and Au layers were of equal thickness and heat treated at 500 °C. XRD analysis on these two samples indicated that the Ni constituent of the Ni/Au films transformed completely into NiO after the heat treatment, while the Au remained in the metallic phase. Our recent cross-sectional TEM observation found that the as-deposited metallic Ni/Au films were reconstructed as a film comprising of a mixture of crystalline NiO, Au, and amorphous Ni–Ga–O phases after being heat treated at 500 °C.[52] A few small voids adjacent to GaN were also found. The as-deposited Au film became discontinuous islands on the top of p-GaN. The NiO formed a continuous film in the outer region which covered the Au islands and amorphous Ni–Ga–O phase. Observation revealed a large percentage of GaN surface area was still in direct contact with NiO. The transformation brought about a specific relationship of crystal orientation between the crystalline NiO, Au islands, and p-GaN. This relationship is NiO(111)//Au(11$\bar{1}$)//GaN(0002) and NiO[$1\bar{1}0$]//Au[$1\bar{1}0$] //GaN[$11\bar{2}0$],[52] as shown in Fig. 4. The NiO and Au were epitaxially formed on p-GaN with sharp interfaces. This process formed a *p-p* isotype heterojunction of GaN and NiO. The reduction of specific contact resistance could be related to the formation of NiO because Au alone could not form low-resistance ohmic contact to p-GaN,[30,31] and the amorphous Ga–Ni–O phase was considered to be insulating currently. Therefore, the minimum value of ρ_c at 500 °C shown in Figs. 3(a) and 3(b) could be due to the optimal phase distribution among NiO and Au. For temperatures below 400 °C, the TEM observation showed the percentage of NiO was not optimized. On the other hand, there was an increase of ρ_c when the temperature was higher than about 600 °C,

Downloaded 08 Apr 2004 to 128.200.94.51. Redistribution subject to AIP license or copyright, see http://jap.aip.org/jap/copyright.jsp

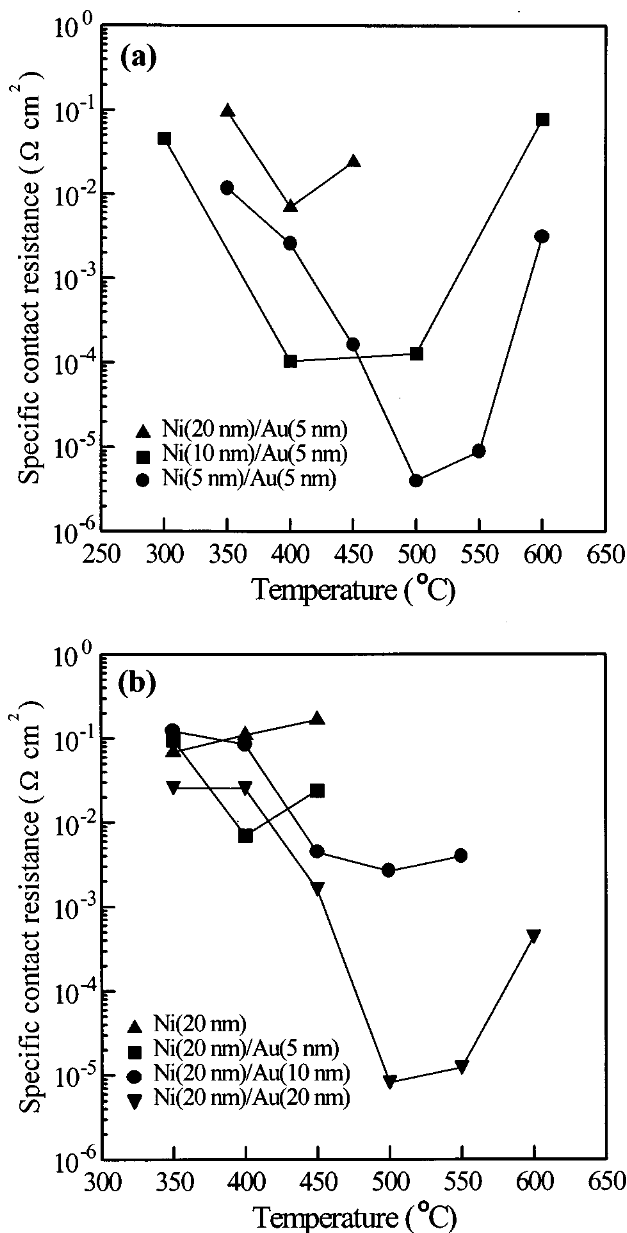

FIG. 3. The effect of heat treatment temperature as well as Ni/Au film thickness on specific contact resistance of Ni/Au contacts to p-GaN heat treated in air. (a) The thickness of Au layer is kept at 5 nm, and (b) the thickness of Ni layer is kept at 20 nm.

due to the fact that oxidized Ni/Au film contained many larger voids and much more amorphous Ni–Ga–O phase. The voids between NiO and p-GaN grew with increasing temperature, separating NiO from p-GaN. This leaves almost only the Au islands in contact with p-GaN. These results hint that the formation of NiO is the reason for obtaining low ρ_c to p-GaN and the amorphous Ni–Ga–O phase may have a detrimental effect.

IV. DISCUSSION

To understand the mechanism for forming low-resistance ohmic contacts, a single Ni film with a thickness of 20 nm was deposited and heat treated in air. The results of ρ_c versus temperature are shown in Fig. 3(b). The oxidized

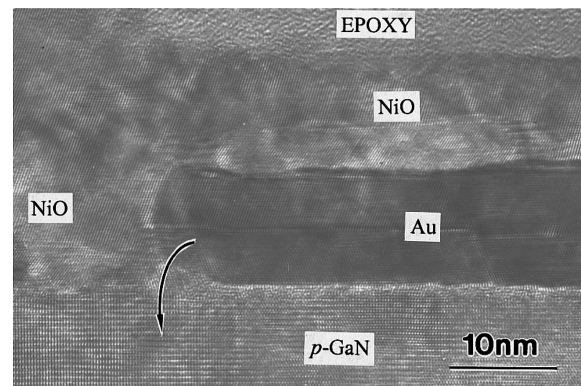

FIG. 4. High resolution TEM image showing the cross-sectional microstructure of oxidized Ni/Au contact to p-GaN. The sample was heat treated at 500 °C in air for 10 min. The arrow indicates a possible low impedance path for current flow.

Ni contacts displayed ohmic characteristics, revealed in the $I-V$ measurements, although the value of ρ_c was high (about $10^{-1}\ \Omega\,\mathrm{cm}^2$). The resistivity of oxidized Ni films was too high to be measured by the conventional four-pointprobe analysis. Once an Au layer was added to the as-deposited Ni films, the oxidized Ni/Au films became conductive. We believe that the Au layer forms islands which disperse in the NiO matrix to enhance the conductivity of oxidized films.[51,52] The presence of Au itself does not necessarily contribute to the reduction of ρ_c for the oxidized Ni/Au ohmic contact.[30,31] Thus the lowering of interface resistance between the oxidized Ni/Au contact and p-GaN can be attributed to the formation of NiO. The high ρ_c for the oxidized Ni contact, compared to those with Au, are due to the high resistivity of the NiO which prevents the current from spreading uniformly over the CTLM contact. The actual contact area for current flow across the interface is much smaller than the nominal circular contact area. Therefore, the real interface impedance could be much lower than the measured value.

The above discussion indicates that the effective configuration of oxidized Ni contact to p-GaN may be regarded as a Au/p-NiO/p-GaN junction since the probes used in $I-V$ measurement are gold plated tungsten needles. Figure 5 displays the equilibrium energy band diagram of the Au/p-NiO/p-GaN junction based on the electron affinity rule.[55] The parameters adopted to construct this energy band diagram, such as energy band gap (E_g), electron affinity (χ), and dielectric constant (ε), etc. are listed in Table I which is explained below. The carrier concentration of p-GaN was measured as $2\times10^{17}\,\mathrm{cm}^3$ by Hall effect measurement. Based on the results of Nakayama *et al.*,[56] the Fermi level is thus located at 0.13 eV above the top of the valence band at 300 K. For NiO, the carrier concentration at 500 °C is estimated to be $1\times10^{16}\,\mathrm{cm}^{-3}$, a figure extrapolated from the high temperature data measured by Peterson and Wiley.[57] The temperature of 500 °C was chosen for the calculation of hole concentration of NiO because the minimum ρ_c is obtained by heat treating at this temperature and then rapidly quenching down to room temperature. Also, the diffusion is negligible at such a temperature.[57] The Fermi level is assessed as about

Downloaded 08 Apr 2004 to 128.200.94.51. Redistribution subject to AIP license or copyright, see http://jap.aip.org/jap/copyright.jsp

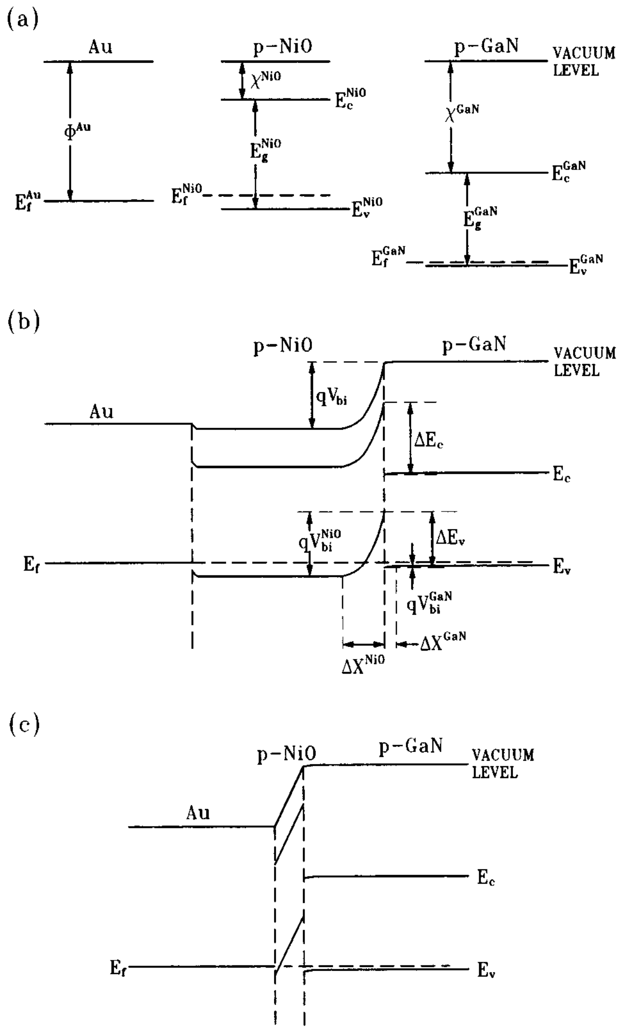

FIG. 5. Estimated equilibrium energy band diagram of (a) bulk Au, p-NiO, and p-GaN, (b) Au/thick p-NiO/p-GaN heterostructure, and (c) Au/thin p-NiO/p-GaN heterostructure.

0.5 eV above the top of the valence band for undoped NiO.[58,59] From these parameters, the conduction band and valence band offsets, ΔE_c and ΔE_v, can be determined to be 2.7 and 2.1 eV, respectively. The total built-in potential (V_{bi}) across the p-NiO/p-GaN isotype heterojunction is assumed to be equal to the work function difference between the p-GaN and p-NiO before any junction is formed. Figure

TABLE I. Properties of p-GaN and p-NiO at room temperature.

Semi-conductor	E_g (eV)	χ (eV)	$E_f - E_v$ (eV)	$[p]$ (cm^{-3})	ε
p-GaN	3.4[a]	4.1[b]	0.13	2×10^{17}	10.4[c]
p-NiO	4.0[d]	1.4[e]	0.5[f]	1×10^{16}	11.9[g]

[a]Reference 61.
[b]References 62 and 63.
[c]Reference 64.
[d]Reference 58.
[e]References 65 and 66.
[f]References 58 and 59.
[g]Reference 67.

TABLE II. Properties of the p-GaN/p-NiO isotype heterojunction based on the electron affinity rule.

ΔE_c (eV)	ΔE_v (eV)	V_{bi} (V)	V_{bi}^{NiO} (V)	V_{bi}^{GaN} (V)	ΔX^{NiO} (nm)	ΔX^{GaN} (nm)
2.7	2.1	2.47	2.415	0.055	571	38

5(a) displays that $V_{bi} = 2.47$ V which is equal to the sum of the partial built-in potentials in p-GaN and p-NiO, respectively, as indicated in Eq. (3)

$$V_{bi} = V_{bi}^{GaN} + V_{bi}^{NiO}, \tag{3}$$

where V_{bi}^{GaN} and V_{bi}^{NiO} are the potentials induced at equilibrium in p-GaN and p-NiO, respectively. Following Cserveny's concept,[60] the relationship between V_{bi}^{GaN} and V_{bi}^{NiO} is derived as

$$\frac{\exp\left(\frac{-qV_{bi}^{NiO}}{kT}\right) + \frac{qV_{bi}^{NiO}}{kT} - 1}{\exp\left(\frac{qV_{bi}^{GaN}}{kT}\right) - \frac{qV_{bi}^{GaN}}{kT} - 1} = \frac{[p]^{GaN}\cdot\varepsilon^{GaN}}{[p]^{NiO}\cdot\varepsilon^{NiO}}, \tag{4}$$

where $[p]$ is the hole concentration, k the Boltzmann constant, q the electronic charge, and T absolute temperature. Here, the hole concentration is used to replace the dopant concentration. V_{bi}^{GaN} and V_{bi}^{NiO} can be obtained by combining Eqs. (3) and (4) and applying the data shown in Table I. Calculation shows them to be equal to 0.055 and 2.415 V, respectively. Besides, the transition width (ΔX) in p-NiO and p-GaN is derived as Eq. (5)

$$\Delta X = \sqrt{\frac{2\varepsilon\cdot V_{bi}}{q\cdot[p]}}. \tag{5}$$

The above results of p-GaN/p-NiO isotype heterojunction are summarized in Table II. For the interface between Au and p-NiO, an ideal ohmic contact is formed because the work function of Au($\Phi^{Au} = 5.10$ eV) is larger than that of p-NiO (4.9 eV), as shown in Fig. 5(a). For a thick p-NiO connected to p-GaN, the situation resembles that of Fig. 5(b). The p-NiO and p-GaN surface bands bend upwards and downwards, respectively, at the p-GaN/p-NiO interface. A deep notch for holes in p-NiO exists close to p-GaN where great amounts of holes are trapped because the top of the valence band is positioned above the Fermi level. Under forward bias condition, with a current injection into p-GaN from Au as defined herein, holes flowing from p-NiO toward p-GaN encounter a barrier at p-GaN surface resulting from the built-in potential in p-GaN. The barrier height is equal to $(E_f^{GaN} - E_v^{GaN}) + qV_{bi}^{GaN} = 0.185$ eV. The impedance at this interface could be very small because the barrier height is relatively low. The p-NiO/p-GaN interface impedance will abruptly decrease when the applied forward voltage reaches a level where the valence band bottom is higher than the Fermi level of p-NiO at the interface. By further increasing the bias, holes can inject into p-GaN from the notch in p-NiO freely. Meanwhile, a large portion of applied voltage is also consumed in the p-NiO to develop an electrical field there because of its high resistivity. The impedance increases

Downloaded 08 Apr 2004 to 128.200.94.51. Redistribution subject to AIP license or copyright, see http://jap.aip.org/jap/copyright.jsp

with increasing reverse bias because of the barrier and the resistive NiO layer. Consequently, the $I-V$ curves are not considered to be symmetric with respect to applied bias. In addition, the total contact resistance could be unable to reach a very low value when the thickness of the p-NiO layer is greater than ΔX^{NiO}.

In our experiments, the oxidized Ni contact is about 33 nm, i.e., markedly smaller than the calculated value of $\Delta X^{\mathrm{NiO}} = 571$ nm. The electrical property is completely different from that predicted in Fig. 5(b). The energy band diagram is shown in Fig. 5(c). Again, there is a hole notch at the heterojunction because of the large band offset between p-NiO and p-GaN. An additional small barrier exists at the Au/p-NiO interface except that one at p-NiO/p-GaN interface as described previously. The barrier height is 0.3 eV resulting from the band discontinuity at the Au/p-NiO interface. Although the band diagram is more complicated because the interaction between Au and p-GaN cannot be neglected, similar qualitative trends are still valid. With forward bias, holes can easily overcome the barriers by thermionic-field emission to inject into p-GaN from p-NiO When the bias becomes negative, electrons can tunnel through the Au/p-NiO interface barrier and inject into the notch to recombine with holes. The contact resistance could be quite low because the notch provides a recombination center for carriers. This is the reason that the $I-V$ curve is linear for the oxidized Ni contact.

As the above discussion shows, the lowest ρ_c was obtained at 500 °C for the oxidized Ni/Au contact. At this temperature, Au, NiO, and the amorphous Ni–Ga–O phase are present. The contact angle of Au islands to p-GaN is about 120°–140°, developing an Au island undercut edge profile. NiO frequently occupies the undercut space, as shown in Fig. 4. The Au/thin p-NiO/p-GaN model is valid under such condition. The arrow in Fig. 4 indicates an Au/p-NiO/p-GaN region with an ultrathin p-NiO layer. In addition, the Au islands are uniformly distributed in the contact, greatly enhancing its conductivity. Combining these effects produces low-resistance ohmic contacts.

V. SUMMARY

This study has developed an ohmic contact to p-GaN with specific contact resistance as low as $4\times10^{-6}\,\Omega\,\mathrm{cm}^2$ by the oxidation of Ni (5 nm)/Au (5 nm) bilayer film in air or oxygen at 500 °C. The oxidized Ni/Au contact comprises Au, NiO, and amorphous Ni–Ga–O phases. The NiO and Au epitaxially build on p-GaN with sharp interfaces. Finally, we proposed a model based on Au/p-NiO/p-GaN heterostructure to explain the low-resistance ohmic behavior.

ACKNOWLEDGMENTS

The authors would like to thank the Ministry of Economic Affairs of the Republic of China for financially supporting this research under Contract No. 88-EC-2-A-17-0164.

[1] S. Nakamura and G. Fasol, *The Blue Laser Diodes* (Springer, Heidelberg, 1997).
[2] S. Nakamura, T. Mukai, and M. Senoh, Appl. Phys. Lett. **64**, 1687 (1994).
[3] S. Nakamura, M. Senoh, N. Iwasa, S. Nagahama, T. Yamada, and T. Mukai, Jpn. J. Appl. Phys., Part 2 **34**, L1332 (1995).
[4] T. Mukai, D. Morita, and S. Nakamura, J. Cryst. Growth **189/190**, 778 (1998).
[5] T. Mukai, H. Narimatsu, and S. Nakamura, Jpn. J. Appl. Phys., Part 2 **37**, L479 (1998).
[6] G. S. Nakamura, Semicond. Sci. Technol. **14**, R27 (1999).
[7] M. A. Khan, J. N. Kuznia, D. T. Olson, J. M. Van Hove, M. Blasingame, and L. F. Reitz, Appl. Phys. Lett. **60**, 2917 (1992).
[8] K. S. Stevens, M. Kinniburgh, and R. Beresford, Appl. Phys. Lett. **66**, 3518 (1995).
[9] M. A. Khan, J. N. Kuznia, D. T. Olson, M. Blasingame, and A. R. Bhattarai, Appl. Phys. Lett. **63**, 2455 (1993).
[10] W. Yang, T. Nohava, S. Krishnankutty, R. Torreano, S. McPherson, and H. Marsh, Appl. Phys. Lett. **73**, 978 (1998).
[11] M. A. Khan, J. N. Kuznia, A. R. Bhattarai, and D. T. Oslon, Appl. Phys. Lett. **62**, 1786 (1993).
[12] M. A. Khan, J. N. Kuznia, D. T. Olson, W. J. Schaff, J. W. Burm, and M. S. Shur, Appl. Phys. Lett. **65**, 1121 (1994).
[13] Y.-F. Wu, B. P. Keller, P. Fini, S. Keller, T. J. Jenkins, L. T. Kehias, S. P. Denbaars, and U. K. Mishra, IEEE Electron Device Lett. **19**, 50 (1998).
[14] F. Ren, C. R. Abernathy, J. M. Van Hove, P. P. Chow, R. Hickman, J. J. Klaasen, R. F. Kopf, H. Cho, K. B. Jung, J. R. La Roche, R. G. Wilson, J. Han, R. J. Shul, A. G. Baca, and S. J. Pearton, MRS Internet J. Nitride Semicond. Res. **3**, 41 (1998).
[15] Z. Fan, S. N. Mohammad, W. Kim, Ö. Aktas, A. E. Botchkarev, and H. Morkoç, Appl. Phys. Lett. **68**, 1672 (1996).
[16] S. J. Cai, R. Li, Y. L. Chen, L. Wong, W. G. Wu, S. G. Thomas, and K. L. Wang, Electron. Lett. **34**, 2354 (1998).
[17] M. E. Lin, Z. Ma, F. Y. Huang, Z. F. Fan, L. H. Allen, and H. Morkoç, Appl. Phys. Lett. **64**, 1003 (1994).
[18] S. Ruvimov, Z. Liliental-Weber, J. Washburn, K. J. Duxstad, E. E. Haller, Z.-F. Fan, S. N. Mohammad, W. Kim, A. E. Botchkarev, and H. Morkoç, Appl. Phys. Lett. **69**, 1556 (1996).
[19] B. P. Luther, S. E. Mohney, T. N. Jackson, M. A. Khan, Q. Chen, and J. W. Yang, Appl. Phys. Lett. **70**, 57 (1997).
[20] B. P. Luther, S. E. Mohney, J. M. Delucca, and R. F. Karlicek, Jr., J. Electron. Mater. **27**, 196 (1998).
[21] W. Götz, N. M. Johnson, J. Walker, D. P. Bour, and R. A. Street, Appl. Phys. Lett. **68**, 667 (1996).
[22] H. Nakayama, P. Hacke, M. R. H. Khan, T. Detchprohm, K. Hiramatsu, and N. Sawaki, Jpn. J. Appl. Phys., Part 2 **35**, L282 (1996).
[23] H. M. Ng, D. Doppalapudi, D. Korakakis, R. Singh, and T. D. Moustakas, J. Cryst. Growth **349**, 189 (1998).
[24] T. Kim, M. C. Yoo, and T. Kim, Mater. Res. Soc. Symp. Proc. **449**, 1061 (1997).
[25] L. L. Smith, M. D. Bremser, E. P. Carlson, T. W. Weeks, Jr., Y. Huang, M. J. Kim, R. W. Carpenter, and R. F. Davis, Mater. Res. Soc. Symp. Proc. **395**, 861 (1996).
[26] B. Menschubg, C. Liu, B. Rauschenbach, K. Kornitzer, and W. Ritter, Mater. Sci. Eng., B **50**, 105 (1997).
[27] R. G. Wilson, C. B. Vartuli, C. R. Abernathy, S. J. Pearton, and J. M. Zavada, Solid-State Electron. **38**, 1329 (1995).
[28] J. C. Zolper, R. G. Wilson, S. J. Pearton, and R. A. Stall, Appl. Phys. Lett. **68**, 1945 (1996).
[29] M. Rubin, N. Newman, J. S. Chan, T. C. Fu, and J. T. Ross, Appl. Phys. Lett. **64**, 64 (1994).
[30] T. Mori, T. Kozawa, T. Ohwaki, Y. Taga, S. Nagai, S. Yamasaki, S. Asami, N. Shibata, and M. Koike, Appl. Phys. Lett. **69**, 3537 (1996).
[31] L. L. Smith, R. F. Davis, M. J. Kim, R. W. Carpenter, and Y. Huang, J. Mater. Res. **12**, 2249 (1997).
[32] K. V. Vassilevski, M. G. Rastegaeva, A. I. Babanin, I. P. Nikitina, and V. A. Dmitriev, MRS Internet J. Nitride Semicond. Res. **1**, 38 (1996).
[33] Y. Yamaoka, Y. Kaneko, S. Nakagawa, and N. Yamada, *Proceedings of the Second International Conference on Nitride Semiconductors*, Tokushima, Japan, 27–31 October 1997, p. P1–19.
[34] D. J. King, L. Zhang, J. C. Ramer, S. D. Hersee, and L. F. Lester, Mater. Res. Soc. Symp. Proc. **468**, 421 (1997).
[35] T. Kim, M. C. Yoo, and T. Kim, Mater. Res. Soc. Symp. Proc. **449**, 1061 (1997).
[36] H. Ishikawa, S. Kobayashi, Y. Koide, S. Yamasaki, S. Nagai, J. Umezaki,

Downloaded 08 Apr 2004 to 128.200.94.51. Redistribution subject to AIP license or copyright, see http://jap.aip.org/jap/copyright.jsp

M. Koike, and M. Murakami, J. Appl. Phys. **81**, 1315 (1997).
[37] J. T. Trexler, S. J. Pearton, P. H. Holloway, M. G. Mier, K. R. Evans, and R. F. Karlicek, Mater. Res. Soc. Symp. Proc. **449**, 1091 (1997).
[38] T. Kim, J. Khim, S. Chae, and T. Kim, Mater. Res. Soc. Symp. Proc. **468**, 427 (1997).
[39] J. K. Sheu, Y. K. Su, G. C. Chi, P. L. Koh, M. J. Jou, C. M. Chang, C. C. Liu, and W. C. Hung, Appl. Phys. Lett. **74**, 2340 (1999).
[40] J. K. Kim, J.-L. Lee, J. W. Lee, H. E. Shin, Y. J. Park, and T. Kim, Appl. Phys. Lett. **73**, 2953 (1998).
[41] J.-S. Jang, H.-G. Kim, K.-H. Park, C.-S. Um, I.-K. Han, S.-H. Kim, H.-K. Jang, and S.-J. Park, Mater. Res. Soc. Symp. Proc. **482**, 1053 (1998).
[42] J.-S. Jang, I.-S. Chang, T.-Y. Seong, and S.-J. Park, *Proceedings of the Second International Symposium on Blue Laser and Light Emitting Diodes*, Chiba, Japan, 29 September–2 October 1998, p. Tu-P33.
[43] J.-S. Jang, I.-S. Chang, H.-K. Kim, T.-Y. Seong, S. Lee, and S.-J. Park, Appl. Phys. Lett. **74**, 70 (1999).
[44] T. Sands, E. D. Marshall, and L. C. Wang, J. Mater. Res. **3**, 914 (1988).
[45] E. Kaminska, A. Piotrowska, A. Barcz, M. Guziewicz, S. Kasjaniuk, M. D. Bremser, R. F. Davis, E. Dynowska, and S. Kwiatkowski, Mater. Res. Soc. Symp. Proc. **482**, 1077 (1998).
[46] D.-H. Youn, M. Hao, H. Sato, T. Sugahara, Y. Naoi, and S. Sakai, Jpn. J. Appl. Phys., Part 1 **37**, 1768 (1998).
[47] D.-H. Youn, M. Hao, Y. Naoi, S. Mahanty, and S. Sakai, Jpn. J. Appl. Phys., Part 2 **37**, 4667 (1998).
[48] M. Suzuki, T. Kawakami, T. Arai, S. Kobayashi, Y. Koide, T. Uemura, N. Shibata, and M. Murakami, Appl. Phys. Lett. **74**, 275 (1999).
[49] A. Durbha, S. J. Pearton, C. R. Abernathy, J. W. Lee, P. H. Holloway, and F. Ren, J. Vac. Sci. Technol. B **14**, 2582 (1996).
[50] M. E. Lin, F. Y. Huang, and H. Morkoç, Appl. Phys. Lett. **64**, 2557 (1997).
[51] J.-K. Ho, C.-S. Jong, C.-N. Huang, C.-Y. Chen, C. C. Chiu, and K.-K. Shih, Appl. Phys. Lett. **74**, 1275 (1999).
[52] L.-C. Chen, F.-R. Chen, J. J. Kai, L. Chang, J.-K. Ho, C.-S. Jong, C. C. Chiu, C.-N. Huang, C.-Y. Chen, and K.-K. Shih, J. Appl. Phys. (accepted).
[53] G. S. Marlow and M. B. Das, Solid-State Electron. **25**, 91 (1982).
[54] A. J. Willis and A. P. Botha, Thin Solid Films **146**, 15 (1987).
[55] R. L. Anderson, Solid-State Electron. **5**, 341 (1962).
[56] H. Nakayama, P. Hacke, M. R. H. Khan, T. Detchprohm, K. Hiramatsu, and N. Sawaki, Jpn. J. Appl. Phys., Part 2 **35**, L282 (1996).
[57] N. L. Peterson and C. L. Wiley, J. Phys. Chem. Solids **46**, 43 (1985).
[58] S. Hüfner, P. Steiner, I. Sander, F. Reinert, and H. Schmitt, Z. Phys. B **86**, 207 (1992).
[59] S. Adler and J. Feinleib, Phys. Rev. B **2**, 3112 (1970).
[60] S. I. Cserveny, Int. J. Electron. **25**, 65 (1986).
[61] H. P. Maruska and J. J. Tietjen, Appl. Phys. Lett. **15**, 327 (1969).
[62] J. I. Pankove and H. Schade, Appl. Phys. Lett. **25**, 53 (1974).
[63] M. R. H. Khan, T. Detchprohm, P. Hacke, K. Hiramatsu, and N. Sawaki, J. Phys. D **28**, 1169 (1995).
[64] Y. J. Wang, R. Kaplan, H. K. Ng, K. Doverspike, D. K. Gaskill, T. Ikedo, I. Akasaki, and H. Amono, J. Appl. Phys. **79**, 8007 (1996).
[65] F. P. Koffyberg and F. A. Benko, J. Electrochem. Soc. **128**, 2476 (1981).
[66] H. Wu and L.-S. Wang, J. Chem. Phys. **107**, 16 (1997).
[67] K. V. Rao and A. Smakula, J. Appl. Phys. **36**, 2031 (1965).

Downloaded 08 Apr 2004 to 128.200.94.51. Redistribution subject to AIP license or copyright, see http://jap.aip.org/jap/copyright.jsp